

Magnetic ordering in  $CeM_2Si_2$  ( $M = Ag, Au, Pd, Rh$ ) compounds as studied by neutron diffraction

B. H. Grier

*Physics Department, Brookhaven National Laboratory, Upton, New York 11973*J. M. Lawrence,\* V. Murgai,<sup>†</sup> and R. D. Parks*Physics Department, Polytechnic Institute of New York, Brooklyn, New York 11201*

(Received 27 October 1983)

We report the results of neutron-diffraction experiments on  $CeM_2Si_2$  ( $M = Ag, Au, Pd, Rh$ ) which were performed to explore the role of valence fluctuations and  $4f$  hybridization in the magnetic ordering of cerium compounds. All four order antiferromagnetically, the first three exhibiting structures consisting of ferromagnetic layers with moments perpendicular to the layers, which are believed to be characteristic of  $4f$ - $4f$  interactions mediated through hybridization with conduction electrons.  $CePd_2Si_2$  has an anomalously small moment ( $0.62\mu_B$ ) in the ordered state.  $CeAg_2Si_2$  exhibits an incommensurate longitudinal, static magnetization wave with moment and propagation direction along the  $a$  axis. The fourth compound,  $CeRh_2Si_2$ , has the highest known transition temperature (39 K) reported for cerium ordering; it exhibits another second-order transition at 27 K to a complex commensurate structure with modulated moments. The results are discussed in terms of the effects that  $4f$  hybridization can have on ordering.

## I. INTRODUCTION

In cerium compounds exhibiting valence-fluctuation effects<sup>1,2</sup> interesting phenomena can occur when the materials are close to the boundary between magnetic and non-magnetic ground states. Recently superconductivity was reported for  $CeCu_2Si_2$  (Refs. 3 and 4); the Cooper pairing appears to take place in an extremely narrow  $4f$  band. This awakened interest<sup>5</sup> in the properties of other cerium compounds with the formula  $CeM_2Si_2$  and the same crystal structure. Static susceptibility and resistivity measurements showed that for  $M = Au, Ag,$  and  $Pd$  an antiferromagnetic transition occurred near  $T_N = 10$  K; for  $M = Ag$  the ordering appeared to have a small ( $gJ \approx 0.03\mu_B$ ) ferromagnetic component. For  $M = Pd$  (Ref. 5) and  $Cu$  (Refs. 3 and 4) both the large Curie-Weiss parameter  $\Theta$  in susceptibility and Kondo-type resistivity suggested the importance of spin-fluctuation effects which occur near valence instabilities. On the other hand, the lack of lattice-constant anomalies<sup>5</sup> suggests that all of these compounds are trivalent, or only weakly mixed valent. Spin-fluctuation effects are not observed for  $M = Au, Ag,$ <sup>5</sup> or  $Rh$ .<sup>6</sup> For  $CeRh_2Si_2$ ,<sup>6</sup> antiferromagnetism appears to set in at  $T_N = 39$  K which, if due to ordering on the Ce site, represents, to the best of our knowledge, the highest known ordering temperature in a cerium compound. Hence in a single class of related compounds we have the opportunity to study magnetic ordering with and without the presence of strong valence-fluctuation effects.

In performing this study we looked for several related effects which can arise due to strong  $4f$ -conduction-electron hybridization and/or valence fluctuations. These include small ordered moments resulting from the competition between the valence fluctuations and  $4f$ - $4f$  interactions as in  $CeIn_3$ ,<sup>7</sup> spin-density-wave ground states where the magnitude of the  $4f$  moment modulates from

site to site due to the (Kondo-type) coupling of the  $4f$  to the conduction electrons as in  $CeAl_2$ ,<sup>8</sup> quantum critical behavior which occurs when the ordering occurs at a temperature  $T_N$  much smaller than the characteristic Fermi-liquid temperature of the spin system (i.e.,  $T_N \ll T_{sf}$ , where  $T_{sf}$  is the spin-fluctuation temperature, as measured by Curie-Weiss  $\Theta$  or the linewidth in inelastic magnetic neutron scattering. This is believed to be the origin of the suppression of the critical fluctuations and concomitant mean-field behavior in  $CeIn_3$ ,<sup>7,9</sup> and anisotropic  $4f$ - $4f$  coupling mediated by the  $4f$ -conduction-electron exchange. This last effect is manifested in sequences of linearly ordered structures containing antiferromagnetically coupled ferromagnetic layers with moments perpendicular to the layers. Such structures are observed in cerium and uranium pnictides and have been explained<sup>10,11</sup> in terms of such anisotropic coupling. As we shall see, the data are consistent with the existence of all four of these effects, with the caveat that we cannot rule out more conventional explanations.

## II. EXPERIMENTAL TECHNIQUES

All the samples except  $CeAg_2Si_2$  were prepared by arc-melting stoichiometric amounts of the constituents. Mass losses on melting were less than 0.3% for these samples.  $CeAg_2Si_2$  was prepared in the same fashion except that excess Ag ( $\sim 2-3$  at. %) was used to compensate for the high volatility of Ag on heating. Mass losses in the  $CeAg_2Si_2$  samples were between 1.5% and 2.0%. All of the samples were then annealed in vacuum for 4-5 d at 800°C. X-ray diffraction indicated that all the samples except  $CeAg_2Si_2$  were single phase after this treatment. With care the secondary phases in  $CeAg_2Si_2$  (which are primarily elemental Si and Ag precipitates) were reduced to the point where they were unobservable on x-ray traces

although weak impurity lines were still observed in the neutron spectra. The measured room-temperature lattice parameters are given in Table I.

Neutron-diffraction measurements were performed on triple-axis neutron spectrometers at the Brookhaven National Laboratory High Flux Beam Reactor. An incident energy of 14.7 meV was used with collimations of 20', 40', 40', and 40' between the reactor and monochromator, monochromator and sample, sample and analyzer, and analyzer and detector, respectively. Higher-order contamination in the neutron beam was eliminated through the use of a pyrolytic graphite filter. Powdered samples were mounted in either flow or pumped He Dewars or, for  $CeRh_2Si_2$ , in a closed-cycle helium refrigerator. Temperature was controlled to better than 100 mK.

### III. RESULTS

#### A. Crystal structure

The  $CeM_2Si_2$  compounds have the tetragonal  $ThCr_2Si_2$ -type crystal structure with space group  $I4/mmm$  ( $D_{4h}^{17}$ ), which is shown in Fig. 1 along with the atomic coordinates. The cerium atoms form a simple body-centered-tetragonal (bct) sublattice in the  $2a$  positions. The transition-metal atoms are in the  $4d$  positions, and the silicon atoms are in the  $4e$  positions. The bct structure results in nuclear peaks appearing only for  $h + k + l = 2n$ .

The high-temperature spectra, consisting of only nuclear peaks, were fit to the above structure using the Rietveld powder refinement technique.<sup>12</sup> The background used in the fits was estimated at several points from the raw data and held fixed in the refinements. Parameters which were varied include the lattice parameters, silicon position, transition-metal and silicon occupation numbers, an overall Debye-Waller factor, three parameters which determine peak width as a function of angle, an overall scale factor, and the zero point of the spectrometer. The resulting occupation numbers refined to 1 within estimated errors in all cases. The resulting lattice parameters and silicon positions, along with the discrepancy factors, are shown in Table II and a typical fit (for  $CePd_2Si_2$ ) is shown in Fig. 2.

The observed  $R$  values are all much larger than those expected based on statistics alone. The reason for this is not clear. Attempts were made to fit the data to the subgroups of  $I4/mmm$ , but no significant improvement of the  $R$  values was obtained. The possibility of exchange of atoms between the  $M$  and Si sites and stoichiometry variations was also investigated by letting the occupation numbers vary, but with negative results. This difficulty has

TABLE I. Room-temperature lattice parameters as measured by x-ray diffraction.

Sample	$a$ (Å)	$c$ (Å)
$CeAu_2Si_2$	4.32	10.19
$CePd_2Si_2$	4.24	9.88
$CeAg_2Si_2$	4.25	10.66
$CeRh_2Si_2$	4.09	10.18

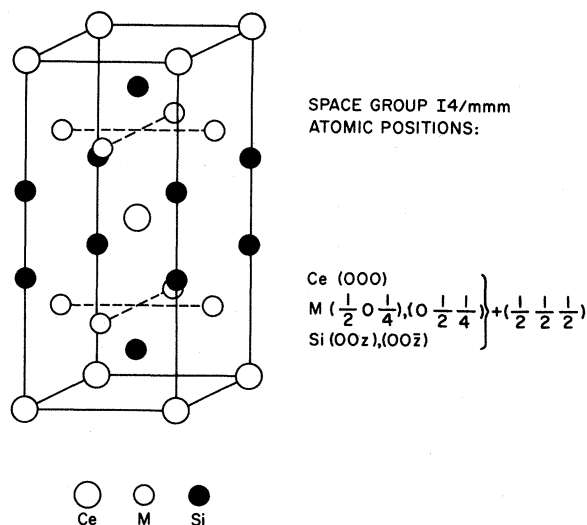


FIG. 1. Crystal structure of the  $CeM_2Si_2$  compounds.

been observed previously in compounds of this structure<sup>13</sup> and has been attributed to preferred orientation or hidden impurity lines.

#### B. Magnetic structures

Below  $T_N$ , all of the compounds show extra peaks which result from the magnetic ordering. Each of the compounds displays a different set of magnetic peaks. The various types of magnetic ordering deduced from these lines are discussed below. The profile refinements used the  $Ce^{3+}$  form factor as calculated by Lander and Brun.<sup>14</sup>

##### 1. $CeAu_2Si_2$

The magnetic lines which appear below  $T_N = 10$  K for  $CeAu_2Si_2$  can all be indexed using the nuclear unit cell and are of the form  $h + k + l = 2n + 1$  with all  $(002n + 1)$  reflections absent. This suggests a simple antiferromagnetic structure with the corner atoms in the unit cell spin up and the body center atom spin down, with the spins along the  $c$  axis. The spin configuration is shown in Fig. 3(a). The results of the profile refinement at 5 K are given in Table II and shown in Fig. 4, where the magnetic peaks are labeled with an  $M$ . The intensities of the  $(100)$ ,  $(102)$ , and  $(111)$  magnetic reflections were measured at a series of temperatures below  $T_N$ , and they were found to vary proportionally to one another, showing that there is no change in the structure below  $T_N$ . This ordering is similar to that in  $ErCo_2Si_2$ ,<sup>13</sup> except that in the case of  $ErCo_2Si_2$  the spins are not along the  $c$  direction. The resulting structure of  $CeAu_2Si_2$  consists of ferromagnetic  $c$  planes with the spins perpendicular to the planes and alternating in sign along the  $c$  direction. The moment calculated for  $CeAu_2Si_2$  at 5 K is  $(1.29 \pm 0.05)\mu_B$ .

TABLE II. Results of the profile refinements. The parameter  $z$  refers to the Si position within the unit cell. In addition to the parameters shown, several instrumental parameters were also refined.  $R$  is a measure of the goodness of fit and  $R = 100 \sum |I(\text{obs}) - I(\text{calc})| / \sum I(\text{obs})$ , where  $I$  is the integrated intensity under a Bragg peak.  $R_{\text{wp}}$  is another indicator of the goodness of fit, calculated point by point and weighted by the standard deviation of the data.  $R_{\text{expt}}$  is the expected value of  $R_{\text{wp}}$  based on statistics,  $R_{\text{wp}}^2 / R_{\text{expt}}^2 = \chi^2$ .

Compound	$T$ (K)	$a$ (Å)	$c$ (Å)	$z$	$T_N$ (K)	$gJ$ ( $\mu_B$ )	$R$ (%)	$R_{\text{wp}}$ (%)	$R_{\text{expt}}$ (%)
CeAu <sub>2</sub> Si <sub>2</sub>	15	4.3002(8)	10.2106(24)	0.3876(7)			4.24	9.96	4.99
	5	4.3005(8)	10.2116(21)	0.3877(7)	10	1.29(5)	4.03	11.70	6.45
CePd <sub>2</sub> Si <sub>2</sub>	15	4.2235(5)	9.8971(12)	0.3799(4)			5.96	7.88	1.36
	5	4.2231(3)	9.8962(10)	0.3800(4)	10	0.62(3)	6.19	8.65	1.69
CeAg <sub>2</sub> Si <sub>2</sub>	15	4.2330(2)	10.6342(2)	0.3918(3)	10		4.19	11.59	6.19
CeRh <sub>2</sub> Si <sub>2</sub>	47.5	4.0840(7)	10.1693(15)	0.3739(5)			9.98	10.18	4.19
	32	4.0834(6)	10.1713(15)	0.3741(5)	39	1.28(5)	8.39	10.65	5.09
	10	4.0828(7)	10.1705(14)	0.3737(5)	27	2.39(26)	8.46	15.11	5.97

## 2. CePd<sub>2</sub>Si<sub>2</sub>

CePd<sub>2</sub>Si<sub>2</sub> also orders at  $T_N = 10$  K, but the indexing of the magnetic lines requires doubling of the unit cell in both the  $a$  and  $b$  directions. The magnetic peaks appear at positions displaced from the nuclear peaks by  $\pm(\frac{1}{2}, \frac{1}{2}, 0)$ . The absence of the  $(\frac{1}{2}, \frac{1}{2}, 0)$  peak indicates that the spins are along the [110] direction, resulting in the spin configuration shown projected into the  $c$  plane in Fig. 3(b). The results of the profile refinement using this structure are given in Table II. Like CeAu<sub>2</sub>Si<sub>2</sub>, the spin configuration of CePd<sub>2</sub>Si<sub>2</sub> consists of ferromagnetic planes with the spins perpendicular to the plane and alternating in direction along the spin axis, with the difference that in CePd<sub>2</sub>Si<sub>2</sub> the spin axis is the [110] axis while in CeAu<sub>2</sub>Si<sub>2</sub> it is the [001] axis. The moment calculated for CePd<sub>2</sub>Si<sub>2</sub> is  $(0.62 \pm 0.03)\mu_B$ .

The intensity of the  $(\frac{1}{2}, \frac{1}{2}, 1)$  peak as a function of temperature is shown in Fig. 5(a). The approach to zero at  $T_N$  appears to be linear, which suggests mean-field

behavior, and the tailing of the intensity above  $T_N$  which is characteristic of short-range order (critical scattering from fluctuations above  $T_N$ ) seems to be absent. We searched for critical scattering by two other methods: First we studied the temperature dependence of the intensity at a  $Q$  value slightly different from the value  $Q_0$  of the  $(\frac{1}{2}, \frac{1}{2}, 1)$  peak (but with  $Q - Q_0$  greater than instrumental resolution). This should show a cusp at  $T_N$ , but no temperature dependence was observed above background. We also studied the  $Q$  dependence in the vicinity of  $Q_0$  for a temperature (10.5 K) close to  $T_N$ . In the presence of critical fluctuations a broad maximum is expected at  $Q_0$  (with  $Q$  dependence of polycrystalline-averaged Ornstein-Zernike form), but none was observed above background. Our conclusion is that there is no critical scattering to a level of 1% of the peak intensity at 4.2 K. To give definitive proof of these two features (mean-field behavior and the absence of critical fluctuations) would require studies in single crystals, yet it is clear from the polycrystalline data that the fluctuations are weaker than in more con-

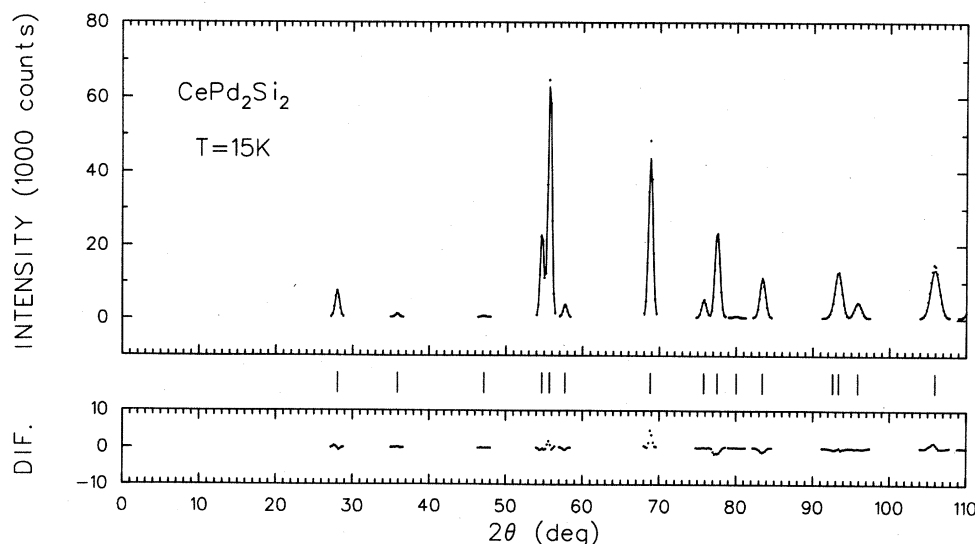


FIG. 2. Results of the profile refinement to the CePd<sub>2</sub>Si<sub>2</sub> data at 15 K. The solid line is the fit, and the dots are the data. The difference is plotted below.

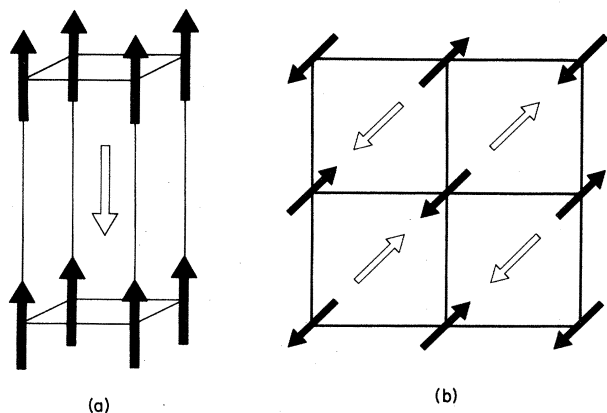


FIG. 3. (a) The magnetic structure of  $CeAu_2Si_2$  at 5 K. (b) The magnetic structure of  $CePd_2Si_2$  at 5 K shown projected into the  $c$  plane.

ventional magnets, such as  $DyPt_3$ .<sup>15</sup>

### 3. $CeAg_2Si_2$

The magnetic lines which appear below  $T_N = 10$  K for  $CeAg_2Si_2$  cannot be indexed in terms of a commensurate magnetic structure. The peaks appear at positions displaced from the nuclear peaks by  $\pm(\delta, 0, 0)$  with  $\delta = 0.685 \pm 0.005$ . Measurements of the  $(1 - \delta 0 1)$  and  $(1 - \delta 1 2)$  peak intensities showed no significant shift in  $\delta$  (to a level of 0.005) between 4.2 and 10 K; at 1.9 K the value of  $\delta$  appears to increase to 0.695. The absence of the  $(\delta 0 0)$  peak indicates that the spins are along the direction of modulation, the  $a$  direction, and rules out helical structures where the moment rotates in the  $a-c$  or  $a-b$  plane.

### 4. $CeRh_2Si_2$

Two magnetic transitions were observed in  $CeRh_2Si_2$ . The first occurs at  $T_N^U = 39$  K, with the appearance of

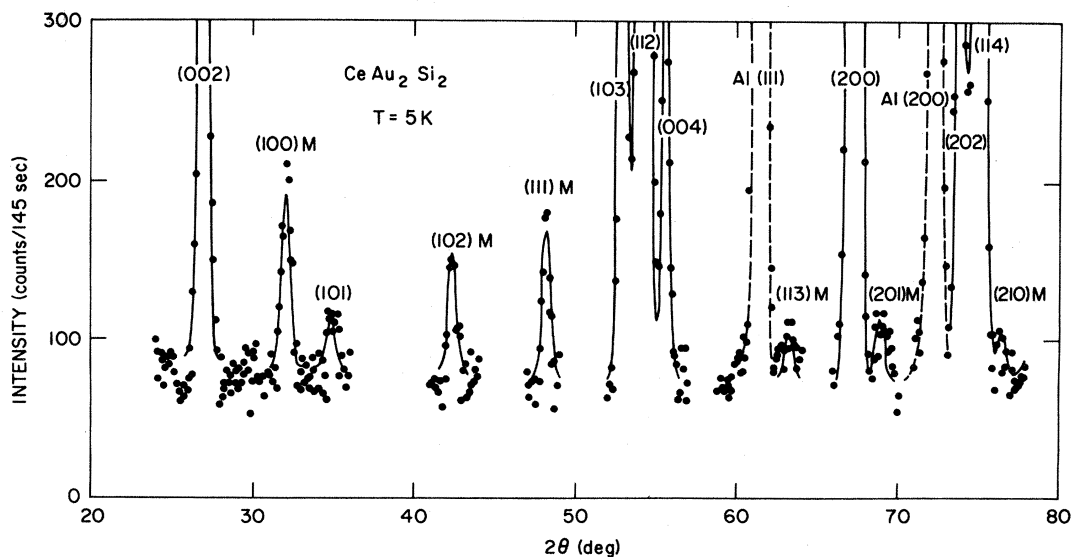


FIG. 4. Results of the profile refinement to the  $CeAu_2Si_2$  data at 5 K. The solid line is the fit to the data, and the dots are the data. The peaks are shown indexed to the nuclear unit cell with the magnetic peaks labeled with an  $M$ . The two Al lines come from the aluminum sample can.

Two types of incommensurate structures are consistent with the data. The first is a modulated moment (spin-density-wave) structure, shown in Fig. 6(a). The second is a square-wave structure which, for  $\delta = 0.685$ , is close to a simple  $++-$  stacking sequence but with occasional anti-phase boundaries. Both structures generate the sequence of peaks  $(h \pm \delta k l)$  (see Table III for a comparison of calculated and observed intensities); the square-wave structure also generates higher odd harmonics, e.g.,  $(h \pm 3\delta k l)$ . The calculated intensity for the third harmonics, which are buried under the  $(h \pm 2k l)$  nuclear peaks, is too small to be detected with the measured statistics. Hence the data cannot distinguish between the two cases; studies in single crystals could resolve this problem. A problem for either interpretation is that the low-angle  $(1 - \delta 0 l)$  peak intensity is too small compared to the calculated value (Table III). A deviation from the  $Ce^{3+}$  form factor at small angles caused by the oppositely polarized conduction electrons around the local cerium moment could account for this discrepancy. The statistics also cannot distinguish the presence of the small ferromagnetic component suggested by the static susceptibility measurements. Again, this magnetic structure consists of ferromagnetic planes with the spins perpendicular to the planes and along the direction of modulation, the  $[100]$  direction this time.

There is no change in the silicon  $z$  parameter above and below  $T_N$  in  $CeAg_2Si_2$ , and the lattice parameters vary smoothly in the transition region. Furthermore, absence of the  $(2 - 2\delta 0 0)$  peak suggests that there is no incommensurate structural distortion accompanying the magnetic transition.

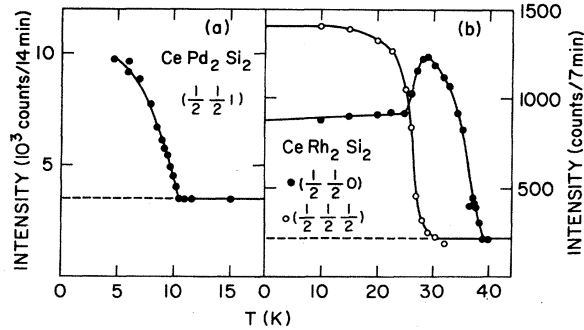


FIG. 5. Temperature dependences of the peak intensities of (a) the  $(\frac{1}{2} \frac{1}{2} 1)$  peak in  $\text{CePd}_2\text{Si}_2$  and (b) the  $(\frac{1}{2} \frac{1}{2} 0)$  and  $(\frac{1}{2} \frac{1}{2} \frac{1}{2})$  peaks in  $\text{CeRh}_2\text{Si}_2$ .

peaks corresponding to a  $(\frac{1}{2} \frac{1}{2} 0)$  magnetic structure. The ratio of the integrated intensity of the  $(\frac{1}{2} \frac{1}{2} 0)$  peak to that of the  $(\frac{1}{2} \frac{1}{2} 2)$  is  $2.6 \pm 0.2$  compared to a calculated ratio of 2.63 for a  $(\frac{1}{2} \frac{1}{2} 0)$  ordering with the spins in the  $c$  direction. This is confirmed by the profile refinement so that the magnetic structure of  $\text{CeRh}_2\text{Si}_2$  is similar to that of  $\text{CePd}_2\text{Si}_2$  shown in Fig. 3(b), but with the spins in the  $c$  direction.

The second transition occurs at  $T_N^L = 27$  K. At this temperature peaks which can be indexed on the basis of a  $(\frac{1}{2} \frac{1}{2} \frac{1}{2})$  magnetic structure appear. The  $(\frac{1}{2} \frac{1}{2} 0)$  peaks begin to decrease as the temperature is lowered, but level off and remain relatively constant below 25 K. The temperature dependences of the  $(\frac{1}{2} \frac{1}{2} \frac{1}{2})$  and  $(\frac{1}{2} \frac{1}{2} 0)$  intensities are shown in Fig. 5(b) and representative scans through this region are shown in Fig. 7. Similar two-magnetic-phase behavior is observed in  $\text{Tb}_2\text{Fe}_3\text{Si}_5$ ,<sup>16</sup> where a commensurate phase and an incommensurate phase are seen to coexist. A profile refinement was performed on the 10 K data with the assumption that the sample is a two-phase mixture with 50% of the sample transforming

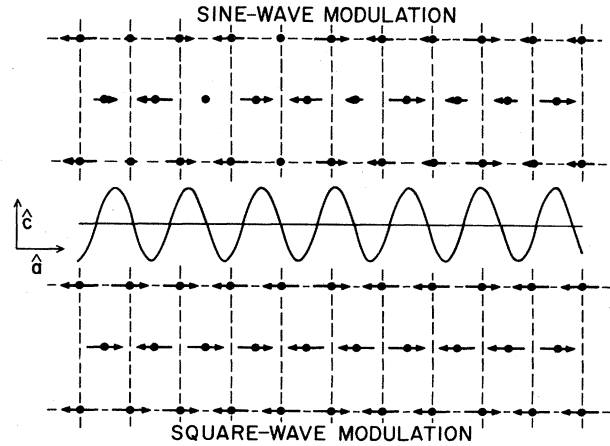


FIG. 6. Two possible magnetic structures for  $\text{CeAg}_2\text{Si}_2$ ; top, sine-wave modulated moment, and bottom, square-wave modulated.

to the  $(\frac{1}{2} \frac{1}{2} \frac{1}{2})$  structure while 50% remains in the  $(\frac{1}{2} \frac{1}{2} 0)$  structure. The results indicate that the spins are in the  $c$  direction in both structures. The moments are  $(2.54 \pm 0.28)\mu_B$  and  $(2.23 \pm 0.23)\mu_B$ , respectively, for the  $(\frac{1}{2} \frac{1}{2} 0)$  and  $(\frac{1}{2} \frac{1}{2} \frac{1}{2})$  domains. Both of these are larger than the maximum of  $2.14 \mu_B$  calculated for the tetragonal crystal-field ground-state moment, and approach the full  $\text{Ce}^{3+}$  free-ion moment of  $2.54\mu_B$ .

The low-temperature ordered structure of  $\text{CeRh}_2\text{Si}_2$  cannot be determined unambiguously from the results. Three interpretations are possible. The first is that the sample is truly two phase at 10 K, with the two different orderings present in two different regions of the sample. This two-phase behavior could result from variations in the vacancy concentration within the sample or from Rh and Si atom interchange in some regions of the sample.

There are several restrictions set on this model by the data. First, the sample must be very close to 50% of each phase at 10 K, since any deviations from this proportion

TABLE III. Calculated and observed magnetic peaks in  $\text{CeAg}_2\text{Si}_2$  using  $a = 4.084 \text{ \AA}$ ,  $c = 10.169 \text{ \AA}$ , and  $\delta = 0.685$ . The  $R$  factor corresponding to these results is 15%.

$h$	$k$	$l$	$2\theta_{\text{calc}}$	$2\theta_{\text{obs}}$	$I_{\text{calc}}$	$I_{\text{obs}}$	$gJ (\mu_B)$	
							Sine wave	Square wave
$1-\delta$	0	1	16.43	16.37	971	$700 \pm 45$	0.72	0.56
$\delta$	0	0	22.23		0	0		
$1-\delta$	1	0	34.32	34.44	532	$574 \pm 49$	0.97	0.76
$\pm\delta$	0	2	34.40					
$1-\delta$	0	3	40.70	40.66	234	$232 \pm 39$	0.99	0.78
$\pm\delta$	1	1	42.09	42.31	340	$375 \pm 68$	1.01	0.79
$1-\delta$	1	2	43.50	43.48	424	$437 \pm 69$	1.02	0.79
$2-\delta$	1	1	57.14	56.82	102	$90 \pm 39$	0.83	0.65
$\pm\delta$	1	3	57.24	57.37	214	$221 \pm 38$	0.98	0.77
$1+\delta$	0	1	58.33	55.50	111	$130 \pm 38$	0.95	0.75
$\pm\delta$	0	4	58.43					
Average							$0.93 \pm 0.10$	$0.73 \pm 0.08$

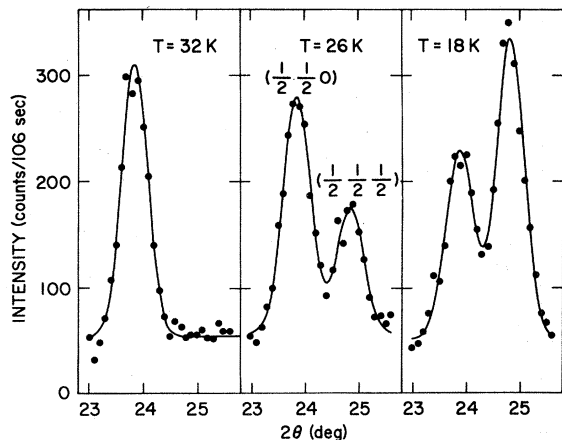


FIG. 7. Raw data showing the  $(\frac{1}{2} \frac{1}{2} 0)$  and  $(\frac{1}{2} \frac{1}{2} \frac{1}{2})$  peaks in  $\text{CeRh}_2\text{Si}_2$  at three different temperatures.

would result in an unacceptably large moment for one of the phases. This large moment could result from a Rh contribution to the ordering, but this is unlikely, as discussed below. Second, at least part of the sample must first order with the  $(\frac{1}{2} \frac{1}{2} 0)$  structure and then, beginning at 27 K, convert to the  $(\frac{1}{2} \frac{1}{2} \frac{1}{2})$  structure at low temperatures. This is apparent from the behavior of the  $(\frac{1}{2} \frac{1}{2} 0)$  peak intensity as a function of temperature [Fig. 5(b)]. This must be reversible since no hysteresis was observed in any of the peaks near  $T = 27$  K.

The second possibility is that both the  $(\frac{1}{2} \frac{1}{2} 0)$  and  $(\frac{1}{2} \frac{1}{2} \frac{1}{2})$  peaks result from a single magnetic phase. This requires that the two structures be superimposed, resulting

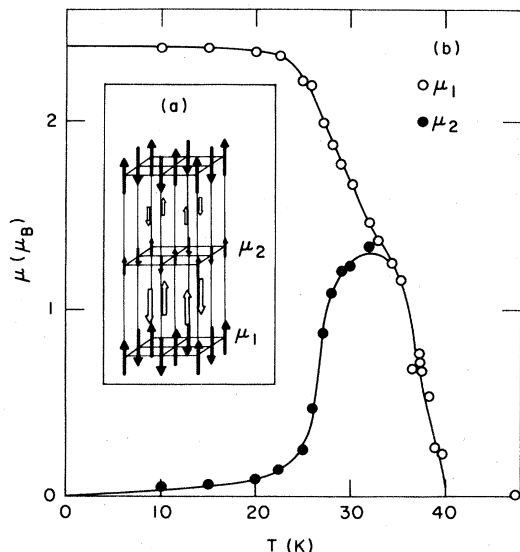


FIG. 8. (a) Possible single-phase magnetic structure of  $\text{CeRh}_2\text{Si}_2$  at 10 K. The large arrows represent a moment of  $2.39\mu_B$  while the smaller ones represent  $0.16\mu_B$ . (b) Two moments in  $\text{CeRh}_2\text{Si}_2$  as a function of temperature as determined from the peak intensities of the  $(\frac{1}{2} \frac{1}{2} 0)$  and  $(\frac{1}{2} \frac{1}{2} \frac{1}{2})$  peaks assuming the structure shown in (a).

in a modulated moment structure with modulation along the  $c$  direction. The structure consists of two  $a$ - $b$  planes with large moment,  $(2.39 \pm 0.26)\mu_B$  at 10 K, in a  $(\frac{1}{2} \frac{1}{2} 0)$  type of arrangement followed by two planes with a weak moment,  $(0.16 \pm 0.26)\mu_B$  at 10 K, in the same ordered structure. This structure is shown in Fig. 8(a). The temperature dependence of the two different sublattice moments are shown in Fig. 8(b), as derived from the intensities of the  $(\frac{1}{2} \frac{1}{2} 0)$  and  $(\frac{1}{2} \frac{1}{2} \frac{1}{2})$  peaks and normalized at 10 K to the refinement results. The behavior is reasonable. This model is free from the constraints discussed above since it requires a single-phase sample and, if the lower transition is second order, no hysteresis is expected. The modulated magnetic structure, however, is rather exotic and requires a mechanism for moment reduction on some of the cerium sites as in  $\text{CeAg}_2\text{Si}_2$ .

The third possibility is that one or both of the magnetic phases observed at 10 K results from ordering on the Rh sites. A most striking feature of the ordering in  $\text{CeRh}_2\text{Si}_2$  is the large value of the ordering temperature ( $T_N = 39$  K). While comparable values occur in one or two nonmetallic compounds such as  $\text{CeBi}$  [ $T_N = 25$  K (Ref. 17)] or  $\text{CeC}_2$  [ $T_N = 33$  K (Ref. 18)], we know of no cerium intermetallics with transition temperatures greater than 10 K. Of course, large transition temperatures can be found in cerium-transition-metal compounds where the ordering occurs on the transition-metal site. A particularly relevant example is the itinerant ferromagnetism observed on the rhodium site in  $\text{CeRh}_3\text{B}_2$  (Ref. 19) with a transition temperature of 115 K. This suggests a similar possibility in the case at hand, i.e., that part of the ordering occurs on the rhodium site. Consistent with this suggestion is the fact that the high-temperature susceptibility of  $\text{CeRh}_2\text{Si}_2$  is enhanced by about 20% over the free-ion value,<sup>6</sup> which could arise from polarization of the Rh  $4d$  bands. The rhodium sites fall on a simple tetragonal lattice with lattice parameters  $a' = a/\sqrt{2}$  and  $c' = c/2$ . Because of this, no simple collinear spin structure can give rise to peaks of the form  $(h \pm \frac{1}{2} k \pm \frac{1}{2} l)$  with both even and odd  $l$  present. The  $(\frac{1}{2} \frac{1}{2} 0)$  ordering is probably not due to rhodium ordering since both even and odd  $l$  peaks were observed with reasonable intensity. The  $(\frac{1}{2} \frac{1}{2} \frac{1}{2})$  ordering is also probably not due to the rhodium atoms for the same reason. In addition, peaks were clearly observed at fairly large values of momentum transfer where the rhodium form factor is expected to be negligible. We are aware of no compounds with the  $\text{ThCr}_2\text{Si}_2$  structure where the magnetic ordering occurs on the transition-metal sublattice. This includes compounds where the transition metal is iron, nickel, or cobalt. The fits to the data assuming ordering on the cerium sublattice with a cerium form factor are very good, and so we believe that we can rule out ordering on the rhodium sites.

The lattice parameters were measured as a function of  $T$  and showed only a smooth variation, in agreement with Ref. 6. Very little change in the intensity of the  $(\frac{1}{2} \frac{1}{2} 0)$  or  $(\frac{1}{2} \frac{1}{2} \frac{1}{2})$  peaks occurs between 10 and 1 K, and there was no indication of any transition at 5.2 K as observed in the static susceptibility measurements.<sup>6</sup> The latter effect may be due to impurities, or it may be field induced.

## IV. DISCUSSION

The magnetic structures exhibited in Sec. III are unusual in several respects: the small ordered moment in  $\text{CePd}_2\text{Si}_2$ , the large transition temperature and modulated moment structure in  $\text{CeRh}_2\text{Si}_2$ , and the incommensurate structure of  $\text{CeAg}_2\text{Si}_2$ . In addition, there is a prevalence of collinearly ordered structures consisting of antiferromagnetically coupled ferromagnetic layers with moments perpendicular to the layers. These findings can all be related to the ideas given in the introduction.

Consider first the small ordered moment ( $0.62\mu_B$ ) observed in  $\text{CePd}_2\text{Si}_2$ . This is comparable to the moment observed in  $\text{CeIn}_3$ ; there are only one or two cerium compounds known to have smaller moments.<sup>7</sup> Indeed, there are several parallels to  $\text{CeIn}_3$ . In both cases large Curie-Weiss parameters  $\Theta \approx 60$  K are observed in the susceptibility and both show extensive regions of Kondo-type negative  $d\rho/dT$  in resistivity. These facts suggest a larger spin-fluctuation temperature  $T_{sf}$ ; for  $\text{CeIn}_3$  this has been measured directly by neutron scattering to be of the order of 100 K.<sup>9</sup> The suggestion is that in both cases the small moment arises from proximity to a zero-temperature magnetic-nonmagnetic instability and that the ordering occurs in the quantum regime where  $T_N \ll T_{sf}$ . It is thus significant that the order parameter for  $\text{CePd}_2\text{Si}_2$  appears to be mean-field-like and that the critical fluctuations are suppressed since these same properties of  $\text{CeIn}_3$  were explained as examples of the quantum critical behavior,<sup>7,9</sup> which is expected due to the dynamics of the  $4f$  spin interacting strongly with the conduction electrons. An important caveat is that the crystal fields expected for this structure<sup>4</sup> could give rise to a large reduction of the moment. We cannot say *a priori* how much moment reduction is due to crystal fields and how much is due to spin fluctuations. However, for  $M=\text{Au}$  ( $1.3\mu_B$ ) and  $\text{Rh}$  ( $2.39\mu_B$ ) the ordered moments are substantially larger. The ground-state moment calculated for  $\text{CeCu}_2\text{Si}_2$ , based on the crystal-field scheme determined from neutron-scattering measurements,<sup>20</sup> is  $(1.3 \pm 0.2)\mu_B$ .  $\text{CeCu}_2\text{Si}_2$  does not order. As such, an ordered moment of  $1.3\mu_B$  gives an indication of the reduction due to crystal fields alone. This, coupled with the other indications of spin-fluctuation effects mentioned above, suggests that our interpretation (that  $\text{CePd}_2\text{Si}_2$  is a reduced-moment antiferromagnet with strong spin fluctuations and  $T_N \ll T_{sf}$ ) is essentially correct.

The fact that for  $M=\text{Pd}$ ,  $\text{Ag}$ , and  $\text{Au}$  the ordered structures consist of ferromagnetic planes with moments perpendicular to the planes and various antiferromagnetic stacking sequences should be considered in light of the ideas of Cooper and co-workers.<sup>10,11</sup> The theory shows that when a  $J = \frac{5}{2}$  moment hybridizes with the conduction electrons, then the  $4f$ - $4f$  interaction mediated through the conduction electrons is highly anisotropic and favors ferromagnetic coupling with moments perpendicular to the interionic axis. Different interionic axes in the crystal compete for this effect with the result that there can be many low-lying collinear structures. These effects have been discussed for the cerium pnictides; the present case is less clearcut due to the lower crystal symmetry

(tetragonal as opposed to cubic). Detailed discussion of these effects also requires knowledge of the crystal-field scheme<sup>20</sup> and measurement of the magnetic anisotropy; e.g., crystal fields can favor certain anisotropy axes. Despite this we can say that the structures are consistent with this mechanism, which is a manifestation of strong  $4f$ -conduction-electron coupling.

The incommensurate structure of  $\text{CeAg}_2\text{Si}_2$  could be one of two possible types. The first possibility is that the structure is of square-wave form. The observed value of incommensuration ( $\delta=0.69$ ) is close to the commensurate case  $\delta = \frac{2}{3}$  ( $++-$  stacking sequence). In the commensurate case the material would be weakly ferrimagnetic; it is possible that the observed weak ferrimagnetism in applied field arises from field-induced transitions to commensurate structures with  $\delta$  values close to 0.7. A structure of this form would be strong confirmation of the anisotropic-interaction hypothesis; indeed, a similar structure (but with  $\delta \approx 0.6$ ) is observed in certain alloys of  $\text{CeBi}$  (Ref. 21) and has been explained in such terms.

The second possibility is that the structure is of the sinusoidal modulated moment form, as observed in  $\text{CeAl}_2$ .<sup>8</sup> Longitudinal sinusoidal modulations have been reported<sup>22</sup> for several heavy rare-earth compounds. The standard explanation is that these structures involve disorder in the perpendicular component and hence must square up at low temperatures. In most cases a first-order transition to a commensurate antiferromagnetic structure is observed at low temperatures.  $\text{CeAl}_2$  is quite different in that the moment modulation seems to persist to zero temperature. This can only be explained as a spin-density wave arising from the Kondo-type coupling of the  $4f$  electrons to the conduction electrons; it represents a particularly exotic many-body problem where the moment is quenched differently at different sites. It would be extremely exciting were  $\text{CeAg}_2\text{Si}_2$  to represent another example of this form of magnetism.

A nearly identical form of ordering occurs in  $\text{UM}_2\text{Si}_2$  compounds.<sup>23</sup> For  $\text{UPd}_2\text{Si}_2$  there is a longitudinal incommensurate structure with both propagation direction and moment direction along the  $c$  axis which undergoes a second transition to a simple antiferromagnet of the  $\text{CeAu}_2\text{Si}_2$  type at a lower temperature. A comparable incommensurate structure in  $\text{UPd}_2\text{Ge}_2$  does *not* become commensurate at 4.2 K. The fact that a similar form of ordering occurs in both Ce-based and U-based structures is consistent with the idea<sup>10,11</sup> that such collinear structures reflect the strong coupling expected between the conduction electrons and the  $4f$  or  $5f$  electrons.

A modulated moment structure also occurs in  $\text{CeRh}_2\text{Si}_2$  at low temperatures with the modulation again along the moment direction. In this case, however, the modulation is commensurate and is superimposed on a  $(\frac{1}{2} \frac{1}{2} 0)$  ordered spin system. The low-temperature structure, which consists of two antiferromagnetic  $a$ - $b$  planes with full moment adjacent to two planes with zero moment, is similar to some of the phases observed in  $\text{CeSb}$  (Ref. 24), where there are planes with zero moment interspersed in various ways with up and down planes with large moment ( $\sim 2\mu_B$ ). This type of structure has also been discussed in terms of Coqblin-Schrieffer-type interactions<sup>25</sup> by

Siemann and Cooper.<sup>10</sup>

A factor arguing against the interpretation of  $CeRh_2Si_2$  and  $CeAg_2Si_2$  in terms of modulated moment ground states is that in both cases neither the resistivity nor the susceptibility show any indication of the spin-fluctuation effects which are seen in the paramagnetic phase of  $CeAl_2$  or  $CePd_2Si_2$  (i.e., the Kondo-type resistivity or large Curie-Weiss parameter  $\Theta$ ). An interesting possibility is that the ordering results in larger spin-fluctuation effects in the ordered phase than in the paramagnetic phase. If the ratios of exchange constants (nearest layer, next-nearest layer, etc.) are such as to reduce the net exchange field to a sufficiently small value at a given layer that the spin-fluctuation energy dominates the exchange energy, the moment would then be reduced at that layer. The anisotropy of the ordered structure could favor stronger  $4f$  hybridization than in the spherically symmetric paramagnetic phase. Neither this case nor its opposite (weaker hybridization below  $T_N$ ) can be ruled out *a priori*; however, enhanced hybridization below  $T_N$  seems consistent with the Cooper-Siemann mechanism,<sup>11</sup> whereby the ordering maximizes  $4f$ - $4f$  covalent bonding.

Finally some observations are in order concerning other causes of and contributions to the observed phenomena. We have already mentioned crystal fields; these cannot only contribute to a reduction of the moment but also to the anisotropies leading to preferred moment directions. While the overall crystal-field scheme in the body-centered-tetragonal structure is known,<sup>20</sup> it is unlikely that calculations of the wave functions for the different cases (i.e., for different transition metals) will soon be available; hence these effects are quite uncertain. The effect of the transition metal on the ordering can be quite large even in heavy rare-earth systems. This can be seen in the  $ErM_2Si_2$  systems where  $ErAu_2Si_2$  orders at 40 K (Ref. 26), while  $ErCo_2Si_2$  orders at 6 K (Ref. 27) and  $ErCu_2Si_2$  fails to order above 4.2 K.<sup>28</sup> Secondly, we expect superexchange to be important for these materials, and it is plausible that the structures could be explained on this basis alone. Thirdly, the Ruderman-Kittel-Kasuya-Yosida mechanism alone could lead to complicated structures due to the sensitivity of the Fermi wave vector to the transition metal

( $M$ ). Finally, mean-field behavior can have other origins besides that of a quantum-critical effect.

## V. CONCLUSION

The neutron-diffraction results for  $CeM_2Si_2$  show a variety of interesting structures which we have discussed in terms of the various consequences of  $4f$ -conduction-electron hybridization. The data, obtained on polycrystalline samples, leaves many questions unanswered, and the role of more conventional effects on the ordering makes the interpretation somewhat ambiguous. Nevertheless, the results are consistent with what we expect from the effect of valence fluctuations on magnetic ordering. Further studies are in order. Neutron studies of single crystals would help clarify the ordering in  $CeAg_2Si_2$  and would allow for unambiguous determination of the critical behavior of  $CePd_2Si_2$  and for examination of the anisotropy of the critical scattering.<sup>29</sup> The latter has made an important contribution to the understanding of the behavior of cerium pnictides. Inelastic neutron scattering would allow determination of crystal fields and, where the valence fluctuations are very strong (as presumably in  $CePd_2Si_2$ ), allow determination of the magnetic quasielastic linewidths,<sup>30</sup> which are a direct measure of the characteristic energy of the spin fluctuations. Finally, polarized beam studies of single crystals could resolve the contribution of the rhodium  $4d$  electrons to the ordering of  $CeRh_2Si_2$ .

## ACKNOWLEDGMENTS

We would like to acknowledge helpful discussions with S. M. Shapiro, A. R. Moodenbaugh, D. E. Cox and B. R. Cooper; we would like to thank G. Shirane, S. M. Shapiro, and D. E. Cox for a critical analysis of this manuscript. A. R. Moodenbaugh also assisted with the profile refinements. The work at Brookhaven National Laboratory was supported by the Division of Materials Sciences, U. S. Department of Energy, under Contract No. DE-AC02-76CH00016, and the work at the Polytechnic Institute of New York was supported by the National Science Foundation under Grant No. DMR-82-02726.

\*Permanent address: Physics Department, University of California, Irvine, CA 92717.

†Present address: Physics Department, Brookhaven National Laboratory, Upton, NY 11973.

<sup>1</sup>*Valence Instabilities*, edited by P. Wachter and H. Boppert (North-Holland, Amsterdam, 1982).

<sup>2</sup>J. M. Lawrence, P. S. Riseborough, and R. D. Parks, *Rep. Prog. Phys.* **44**, 1 (1981).

<sup>3</sup>F. Steglich, J. Aarts, C. D. Bredl, W. Lieke, D. Mesched, W. Franz, and H. Schäfer, *Phys. Rev. Lett.* **43**, 1892 (1979).

<sup>4</sup>W. Lieke, U. Rauchschwalbe, C. D. Bredl, F. Steglich, J. Aarts, and F. R. de Boer, *J. Appl. Phys.* **53**, 2111 (1982).

<sup>5</sup>V. Murgai, S. Raen, L. C. Gupta, and R. D. Parks, in *Valence Instabilities*, Ref. 1, p. 537; see also D. Rossi, R. Marazza, and R. Ferro, *J. Less-Common Met.* **66**, 17 (1979).

<sup>6</sup>C. Godart, L. C. Gupta, and M. F. Ravet-Krill (unpublished).

<sup>7</sup>J. M. Lawrence, *J. Appl. Phys.* **53**, 2117 (1982).

<sup>8</sup>See 2.2.1 of Ref. 2, and works cited therein.

<sup>9</sup>J. M. Lawrence and S. M. Shapiro, *Phys. Rev. B* **22**, 4379 (1980).

<sup>10</sup>R. Siemann and B. R. Cooper, *Phys. Rev. Lett.* **44**, 1015 (1980).

<sup>11</sup>B. R. Cooper and R. Siemann, in *Crystalline Electric Field and Structural Effects in f-Electron Systems*, edited by J. E. Crow, R. P. Guertin, and T. W. Mihalisin (Plenum, New York, 1981), p. 24.

<sup>12</sup>H. M. Rietveld, *J. Appl. Crystallogr.* **2**, 65 (1969).

<sup>13</sup>J. K. Yakinthos, C. H. Routsis, and P. Schobinger-Papamantellos, *J. Magn. Mater.* **30**, 355 (1983).

<sup>14</sup>G. H. Lander and T. O. Brun, *J. Chem. Phys.* **53**, 1387 (1970).

<sup>15</sup>G. Arnold and N. Neresen, *J. Chem. Phys.* **51**, 1495 (1969).

<sup>16</sup>A. R. Moodenbaugh, D. E. Cox, and H. F. Braun, *Phys. Rev. B* **25**, 4702 (1982).

<sup>17</sup>J. W. Cable and W. C. Koehler, in *Magnetism and Magnetic Materials—1971 (Chicago)*, *Proceedings of the 17th Annual Conference on Magnetism and Magnetic Materials*, edited by

- D. C. Graham and J. J. Rhyne (AIP, New York, 1972), p. 1381.
- <sup>18</sup>M. Atoji, *J. Chem. Phys.* **46**, 1891 (1967).
- <sup>19</sup>S. K. Dhar, S. K. Malik, and R. Vijayaraghavan, *J. Phys. C* **14**, L321 (1981).
- <sup>20</sup>S. Horn, E. Holland-Moritz, M. Loewenhaupt, F. Steglich, H. Scheuer, A. Benoit, and J. Flouquet, *Phys. Rev. B* **23**, 3171 (1981).
- <sup>21</sup>G. Meier, W. Hälg, and O. Vogt, *Physica* **86-88B**, B, 121 (1977).
- <sup>22</sup>See, e.g., J. W. Cable, E. O. Wollan, W. C. Koehler, and M. K. Wilkinson, *Phys. Rev.* **140**, 1896 (1965).
- <sup>23</sup>H. Ptasiencz-Bak, J. Leciejewicz, and A. Zygmunt, *J. Phys. F* **11**, 1225 (1982).
- <sup>24</sup>J. Rossat-Mignod, P. Bulet, J. Villain, H. Bartholin, T. S. Wang, and D. Florence, *Phys. Rev. B* **16**, 440 (1977); P. Fischer, B. Lebech, G. Meier, B. D. Rainford, and O. Vogt, *J. Phys. C* **11**, 345 (1978).
- <sup>25</sup>B. Coqblin and J. R. Schrieffer, *Phys. Rev.* **185**, 847 (1969).
- <sup>26</sup>I. Felner, *J. Phys. Chem. Solids* **36**, 1063 (1975).
- <sup>27</sup>J. K. Yakinthos, Ch. Rontsi, and P. F. Ikonou, *J. Less-Common Met.* **72**, 205 (1980).
- <sup>28</sup>P. A. Kotsanidis and J. K. Yakinthos, *Solid State Commun.* **40**, 1041 (1981).
- <sup>29</sup>S. K. Sinha, G. H. Lander, S. M. Shapiro, and O. Vogt, *Phys. Rev. Lett.* **45**, 1028 (1980).
- <sup>30</sup>B. H. Grier, R. D. Parks, S. M. Shapiro, and C. F. Majkrzak, *Phys. Rev. B* **24**, 6242 (1981).